

¹ **The Morphological Diversification of Siphonophore Tentilla**

³ Alejandro Damian-Serrano^{1,‡}, Steven H.D. Haddock², Casey W. Dunn¹

⁴ ¹ Yale University, Department of Ecology and Evolutionary Biology, 165 Prospect St.,
⁵ New Haven, CT 06520, USA

⁶ ² Monterey Bay Aquarium Research Institute, 7700 Sandholdt Rd., Moss Landing, CA
⁷ 95039, USA

⁸ [‡] Corresponding author: Alejandro Damian-Serrano, email: alejandro.damianserrano@
⁹ yale.edu

¹⁰ **Abstract**

¹¹ Siphonophore tentilla (tentacle side branches) are unique biological structures for prey capture,
¹² composed of a complex arrangement of cnidocytes (stinging cells) bearing different types
¹³ of nematocysts (stinging capsules) and auxiliary structures. Tentilla present an exuberant
¹⁴ morphological diversity of form and function across species. While associations between
¹⁵ tentilla form and diet have been reported, the evolutionary history giving rise to this
¹⁶ morphological diversity is largely unexplored. Here we explore the evolutionary gains and
¹⁷ losses of novel tentillum substructures and nematocyst types on the most recent siphonophore
¹⁸ phylogeny. Tentilla have a precisely coordinated high-speed strike mechanism of synchronous
¹⁹ unwinding and nematocysts discharge. Here we characterize the kinematic diversity of this
²⁰ prey capture reaction using high-speed video and find relationships with morphological
²¹ characters. Since tentillum discharge occurs in synchrony across a broad morphological
²² diversity, we evaluate how phenotypic integration is maintaining character correlations across
²³ evolutionary time. Moreover, we analyze the dimensionality of the tentillum morphospace,
²⁴ identify instances of heterochrony and morphological convergence, and generate hypotheses
²⁵ on the diets of understudied siphonophore species. Our findings indicate that siphonophore

26 tentilla are phenotypically integrated structures with a complex evolutionary history leading to
27 a phylogenetically structured diversity of forms which are predictive of kinematic performance
28 and feeding habits.

29 **Keywords**

30 Siphonophore, tentilla, nematocysts, character evolution

31 **Introduction**

32 Siphonophores have fascinated zoologists for centuries for their extremely subspecialized
33 colonial organization and integration. Today we hold more knowledge than ever on the
34 morphological diversity of this group due to the extensive work of siphonophore taxonomists
35 in the past few decades (1–10), which has been elegantly synthesized in detailed synopsis (11).
36 In addition, recent advances in phylogenetic analyses of siphonophores (13, 14) have provided
37 a macroevolutionary context to interpret this diversity. With these assets in hand, we can
38 now begin to study siphonophores from an orthogonal perspective, focusing on the diversity
39 and evolutionary history of specific structures. Here we focus on one of such structures: the
40 tentilla. Like many cnidarians, siphonophore tentacles bear side branches (tentilla) with
41 nematocysts. But unlike other cnidarians, most siphonophore tentilla are dynamic structures
42 that react to prey encounters by shooting the nematocyst battery to slap around the prey.
43 This maximizes the surface area of contact between the nematocysts and the prey they fire
44 upon. In addition, siphonophore tentilla present a remarkable diversity of morphologies, sizes,
45 and nematocyst complements (Fig. 1). Our overarching aim is to organize all this phenotypic
46 diversity in a phylogenetic context, and identify the evolutionary processes that generated it.

47 In (14), we collected the most extensive morphological dataset on siphonophore tentilla
48 and nematocysts using state-of-the-art microscopy techniques, and expanded the taxon
49 sampling of the phylogeny to disentangle the evolutionary history. The analyses we carried
50 out led to novel, generalizable insights into the evolution of predatory specialization. The

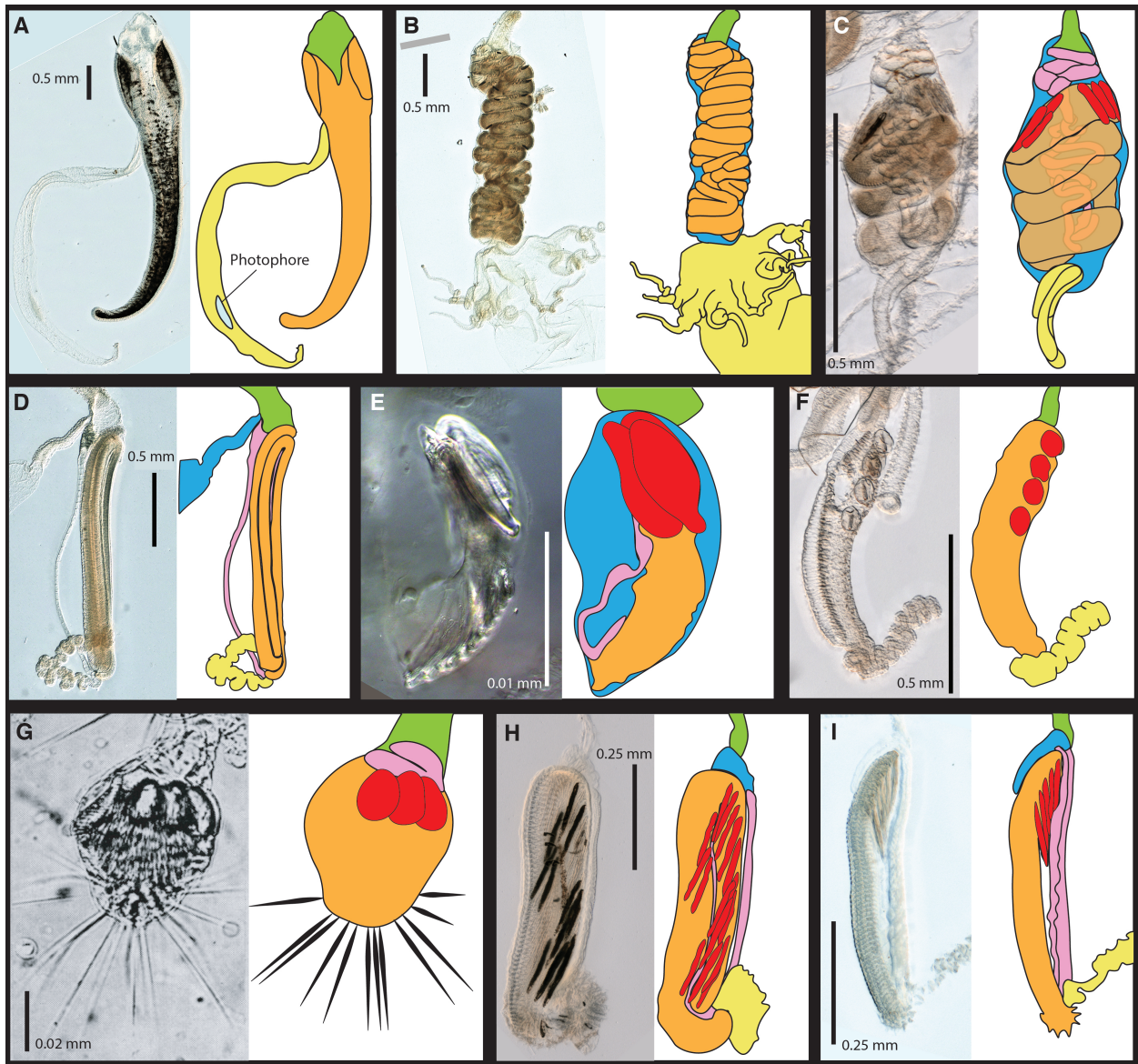


Figure 1: Tentillum diversity. The illustrations delineate the pedicle (green), involucrum (blue), cnidoband (orange), elastic strands (pink), terminal structures (yellow). Heteroneme nematocysts (stenoteles in C,E,F,G and mastigophores in H,I) are depicted in red for some species. A - *Erenna laciniata*, 10x. B - *Lychnagalma utricularia*, 10x. C - *Agalma elegans*, 10x. D - *Resomia ornicephala*, 10x. E - *Frillagalma vityazi*, 20x. F - *Bargmannia amoena*, 10x. G - *Cordagalma* sp., reproduced from Carré 1968. H - *Lilyopsis fluoracantha*, 20x. I - *Abylopsis tetragona*, 20x.

51 work we present here is complementary to (14), showcasing a far more detailed account on
52 the evolutionary history of tentilla morphology.

53 Nematocysts are unique biological weapons for defense and prey capture exclusive to
54 the phylum Cnidaria. Mariscal ((15)) reported that hydrozoans have the largest diversity
55 of nematocyst types among cnidarians. Among them, siphonophores present the greatest
56 variety of types (12), and vary widely across taxa in which and how many types they carry
57 on their tentacles. Werner (???) noted that there are nine types of nematocyst found
58 in siphonophores, of which four, anacrophore & acrophore rhopalonemes, homotrichous
59 anisorrhizas, and birhopaloids are unique to them. Heteroneme and haploneme nematocysts
60 serve penetrant and entangling functions, while rhopalonemes and desmonemes work by
61 adhering to the surface of the prey. While recent descriptive studies have expanded and
62 confirmed our understanding of this diversity, the evolutionary history of nematocyst type
63 gain and loss in siphonophores remains unexplored. Thus, here we reconstruct the evolution
64 of shifts, gains, and losses of nematocyst types, subtypes, and other major categorical traits
65 that led to the extant diversity we see in siphonophore tentilla.

66 In (14) we fitted discriminant analyses to identify characters that are predictive of feeding
67 guild. These discriminant analyses can be used to generate hypotheses on the diets of
68 ecologically understudied siphonophore species for which we have morphology data. Here
69 we present a Bayesian prediction for the feeding guild of 45 species using the morphological
70 dataset in (14). As mentioned above, tentilla are far from being ornamental shapes and are
71 in fact violently reactive weapons for prey capture (14, 16). While we now have detailed
72 characterizations of tentilla morphologies across many species, the diversity of dynamic
73 performances and their relationships to the undischarged morphologies have not been examined
74 to date. To address this gap, we set out to record high-speed video of the *in vivo* discharge
75 dynamics of several siphonophore species at sea, and compare the kinematic attributes to
76 their morphological characters.

77 **Methods**

78 All character data and the phylogeny analyzed here were published in (14). We log transformed
79 all the continuous characters that did not pass Shapiro-Wilks normality tests, and used
80 the ultrametric constrained Bayesian time tree in all comparative analyses. When missing
81 data was incorporated as inapplicable states, we removed those species with characters that
82 could not be measured due to technical limitations. We used the feeding guild categories
83 detailed in (14) with one modification: including all *Forskalia* spp. as generalists not only
84 a single *Forskalia* species on the tree after a reinterpretation of the data in (17). In order
85 to characterize the evolutionary history of tentilla morphology, we fitted different models
86 generating the observed data distribution given the phylogeny for each continuous character
87 using the function `fitContinuous` in the R package *geiger* (18). These models include a
88 non-phylogenetic white-noise model (WN), a neutral divergence Brownian Motion model
89 (BM), an early-burst decreasing rate model (EB), and an Ornstein-Uhlenbeck (OU) model
90 with stabilizing selection around a fitted optimum trait value. In the same way as (14) we
91 then ordered the models by increasing parametric complexity (WN, BM, EB, OU), and
92 compared their corrected Akaike Information Criterion (AICc) scores (19). We used the
93 lowest (best) score using a delta cutoff of 2 units to determine significance relative to the
94 next simplest model (SM10). We calculated model adequacy scores using the R package
95 *arbutus* (20) (SM11). We calculated phylogenetic signals in each of the measured characters
96 using Blomberg's K (21) (SM10). To reconstruct the ancestral character states of nematocyst
97 types and other categorical traits, we use stochastic character mapping (SIMMAP) using the
98 package *phytools* (22).

99 In order to examine the phenotypic integration in the tentillum, we explored the correla-
100 tional structure among continuous characters and among their evolutionary histories using
101 principal component analysis (PCA) and phylogenetic PCA (22). Since the character dataset
102 contains many gaps due to missing characters and inapplicable states, we carried out these
103 analyses on a subset of species and characters that allowed for the most complete dataset.

104 This was done by removing the terminal filament characters (which are only shared by a small
105 subset of species), and then removing species which had inapplicable states for the remaining
106 characters (apolemiids and cystonects). In addition, we obtained the correlations between
107 the phylogenetic independent contrasts (23) using the package *rphylip* (24). We identified
108 four hypothetical modules among the tentillum characters: (1) The tentillum scaffold module
109 – cnidoband length & width, nematocyst row number, pedicle & elastic strand width, tentacle
110 width; (2) the heteroneme module – heteroneme length & width, shafts length & width; (3)
111 the haploneme module – length and width; and (4) the terminal filament module – desmoneme
112 & rhopaloneme length & width. To test and quantify phenotypic integration between these
113 multivariate modules, we used the phylogenetic phenotypic integration test in the package
114 *geomorph* (25).

115 When looking at the morphospace of species in different feeding guilds, we also used
116 PCA on the complete tentacular character dataset transforming inapplicable states of absent
117 characters to zeros to account for similarity based on character presence/absence. Using
118 these principal components, we examined the occupation of the morphospace across species
119 in different feeding guilds using a phylogenetic MANOVA with the package *geiger* (18) to
120 assess the variation explained, and a morphological disparity test with the package *geomorph*
121 (25) to assess differences in the extent occupied by each guild.

122 In order to detect and evaluate instances of convergent evolution, we used the package
123 SURFACE (26). This tool identifies OU regimes and their optima given a tree and character
124 data, and then evaluates where the same regime has appeared independently in different
125 lineages. We applied these analyses to the haploneme nematocyst length and width characters
126 as well as to the most complete dataset without inapplicable character states.

127 In order to generate hypotheses on the diets of siphonophores using tentilla morphology,
128 we used the discriminant analyses of principal components (DAPC) (27) trained in (14) to
129 predict the feeding guilds of species in the dataset for which there are no published feeding
130 observations.

¹³¹ In order to observe the discharge behavior of different tentilla, we recorded high speed
¹³² footage (1000-3000 fps) of tentillum and nematocyst discharge by live siphonophore specimens
¹³³ (26 species) using a Phantom Miro 320S camera mounted on a stereoscopic microscope. We
¹³⁴ mechanically elicited tentillum and nematocyst discharge using a fine metallic pin. We used
¹³⁵ the Phantom PCC software to analyze the footage. For the 10 species recorded, we measured
¹³⁶ total cnidoband discharge time (ms), heteroneme filament length (μm), and discharge speeds
¹³⁷ (mm/s) for cnidoband, heteronemes, haplonemes, and heteroneme shafts when possible (data
¹³⁸ available in the Dryad repository).

¹³⁹ Results

¹⁴⁰ *Evolutionary history of tentillum morphology* – In (14), we produced the most speciose
¹⁴¹ siphonophore molecular phylogeny to date, while incorporating the most recent findings
¹⁴² in siphonophore deep node relationships. This phylogeny revealed for the first time that
¹⁴³ the genus *Erenna* is the sister to *Stephanomia amphytridis*. *Erenna* and *Stephanomia* bear
¹⁴⁴ the largest tentilla among all siphonophores, thus their monophyly indicates that there was
¹⁴⁵ a single evolutionary transition to giant tentilla. Siphonophore tentilla range in size from
¹⁴⁶ ~30 μm in some *Cordagalma* specimens to 2-4 cm in *Erenna* species, and up to 8 cm in
¹⁴⁷ *Stephanomia amphytridis* (10). Most siphonophore tentilla measure between 175 and 1007
¹⁴⁸ μm (1st and 3rd quartiles), with a median of 373 μm . The extreme gain of tentillum size in
¹⁴⁹ this newly found clade may have important implications for access to large prey size classes
¹⁵⁰ such as adult deep-sea fishes.

¹⁵¹ Siphonophore tentilla are defined as lateral, monostichous evaginations of the tentacle
¹⁵² gastrovascular lumen with epidermal nematocysts (11). The buttons on *Physalia* tentacles
¹⁵³ were not traditionally regarded as tentilla, but (8) and our observations (13), confirm
¹⁵⁴ that the buttons contain evaginations of the gastrovascular lumen, thus satisfying all the
¹⁵⁵ criteria for the definition. In this light, and given that most Cystonectae bear conspicuous
¹⁵⁶ tentilla, we conclude (in agreement with (13) and (14)) that tentilla are likely ancestral to

157 all siphonophores, and secondarily lost twice, once in *Apolemia* and again in *Bathyphysa*
158 *conifera*.

159 In order to gain a broad perspective on the evolutionary history of tentilla, we reconstructed
160 the phylogenetic positions of the main categorical character shifts using stochastic character
161 mapping (SM1-9) and summarized in (Fig. 2). Some of these characters include the gain
162 and loss of nematocyst types. Based on external information, we assume that haploneme
163 nematocysts are ancestrally present in siphonophore tentacles since they are present in the
164 tentacles of many other hydrozoans (15). Haplonemes first diverged into spherical isorhizas
165 of 2 size classes in Cystonectae, and elongated anisorrhizas of one size class in Codonophora.
166 Haplonemes were likely lost in the tentacles of *Apolemia* but retained as spherical isorhizas in
167 other *Apolemia* tissues (28). Similarly, while heteronemes exist in other tissues of cystonects,
168 they appear in the tentacles of codonophorans exclusively, as birhopaloids in *Apolemia*,
169 stenoteles in eucladophoran physonects, and microbasic mastigophores in calycophorans.
170 The four nematocyst types unique to siphonophores appear in two events in the phylogeny
171 (Fig. /???(figure7)): birhopaloids evolved in the stem to *Apolemia*, while rhopalonemes
172 (acrophore and anacrophore) as well as homotrichous anisorrhizas evolved in the branch
173 leading to Tendiculophora. Nematocyst type gain and loss is also associated with prey
174 capture functions. For example, the loss of desmonemes and rhopalonemes in piscivorous
175 *Erenna*, retaining solely the penetrant (and venom injecting) anisothizas and stenoteles (two
176 size classes) is reminiscent of the two size classes of penetrant isorhizas in the fish-specialist
177 cystonects. Moreover, with the gain of anisorrhizas, desmonemes, and rhopalonemes, the
178 Tendiculophora gained versatility in entangling and adhesive functions of the cnidoband and
179 terminal filament, allowing specializations to evolve into the generalist, shrimp-specialist,
180 and fish-specialist Euphysonects and the more crustacean-specialized calycophorans. Part of
181 the success of calycophoran cnidobands at entangling crustaceans may be attributed to the
182 subspecialization of their heteronemes. These shifted from the ancestral penetrating stenotele
183 to the microbasic mastigophore (or eurytele in some species) with a long barbed shaft with

many long spines. This heteroneme subtype could arguably be better at interlocking with the setae of crustacean legs and antennae. In those species that have a functional terminal filament, the desmonemes and rhopalonemes play a fundamental role in the first stages of adhesion of the prey. In many species, the tugs of the struggling prey on the terminal filament trigger the cnidoband discharge (16). The adhesive terminal filament has been lost several times in the Euphysonectae (*Frillagalma*, *Lychnagalma-Physophora*, *Erenna*, and some species of *Cordagalma*). In these species, we hypothesize that a different trigger mechanism is at play, possibly involving the prey actively biting or grasping the tentillum or lure.

The clades defined in (14) are characterized by unique evolutionary innovations in their tentilla. The clade Eucladophora (containing Pyrostephidae, Euphysonectae, and Calycophorae) encompasses all of the extant Siphonophore species (178 of 186) except Cystonects and *Apolemia*. Innovations that arose along the stem of this group include spatially segregated heteroneme and haploneme nematocysts, terminal filaments, and elastic strands (Fig. 2). Pyrostephids evolved a unique bifurcation of the axial gastrovascular canal of the tentillum known as the “saccus” (11). The stem to the clade Tendiculophora (clade containing Euphysonectae and Calycophorae) subsequently acquired further novelties such as the desmoneme and rhopaloneme (acrophore subtype ancestral) nematocysts on the terminal filament (Fig. 2), which bears no other nematocyst type. These are arranged in sets of 2 parallel rhopalonemes for each single desmoneme (29, 30). The involucrum is an expansion of the epidermal layer that can cover part or all of the cnidoband (Fig. 1). This structure, together with differentiated larval tentilla, appeared in the stem branch to Clade A physonects. Calycophorans evolved novelties such as larger desmonemes at the distal end of the cnidoband, pleated pedicles with a “hood” (here considered homologous to the involucrum) at the proximal end of the tentillum, anacrophore rhopalonemes, and microbasic mastigophore-type heteronemes. While calycophorans have diversified into most of the extant described siphonophore species (108 of 186), their tentilla have not undergone any major categorical gains or losses since their most recent common ancestor. Nonetheless,

211 they have evolved a wide variation in nematocyst and cnidoband sizes. Ancestrally (and
212 retained in most prayomorphs and hippopodids), the calycophoran tentillum is recurved
213 where the proximal and distal ends of the cnidoband are close together. Diphyomorph tentilla
214 are slightly different in shape, with straighter cnidobands.

215 *Evolution of tentillum and nematocyst characters* – One-third of the characters measured
216 in (14) support a non-phylogenetic generative model, indicating they are not phylogenetically
217 conserved (SM10). Most (74%) characters present a significant phylogenetic signal, yet only
218 total nematocyst volume, haploneme length, and heteroneme-to-cnidoband length ratio had
219 a phylogenetic signal with K larger than 1. Total nematocyst volume and cnidoband-to-
220 heteroneme length ratio showed strongly conserved phylogenetic signals. The majority (67%)
221 of characters support BM models, indicating a history of neutral constant divergence. We did
222 not find any relationship between phylogenetic signal and BM model support. Haploneme
223 nematocyst length was the only character with support for an EB model of decreasing rate
224 of evolution with time. No character had support for a single-optimum OU model (when not
225 informed by feeding guild regime priors). The model adequacy tests (SM11) indicate that
226 many characters may have a relationship between the states and the rates of evolution (Sasr)
227 not captured in the basic models compared here, accompanied by a signal of unaccounted
228 rate heterogeneity (Cvar). No characters show significant deviations in the overall rate of
229 evolution estimated (Msig). Some characters show a perfect fit (no significant deviations
230 across all metrics) under BM evolution, such as heteroneme shape, length, width & volume,
231 haploneme width & SA/V, tentacle width and pedicle width. Haploneme row number and
232 rhopaloneme shape have significant deviations across four metrics, indicating that BM (best
233 model) is a poor fit. These characters likely evolved under complex models which would
234 require many more data points than we have available to fit with accuracy.

235 *Evolution of nematocyst shape* – The greatest evolutionary change in haploneme nemato-
236 cyst shape occurred in a single shift towards elongation in the stem of Tendiculophora, which
237 contains the majority of described siphonophore species other than *Cystonects*, *Apolemia*,

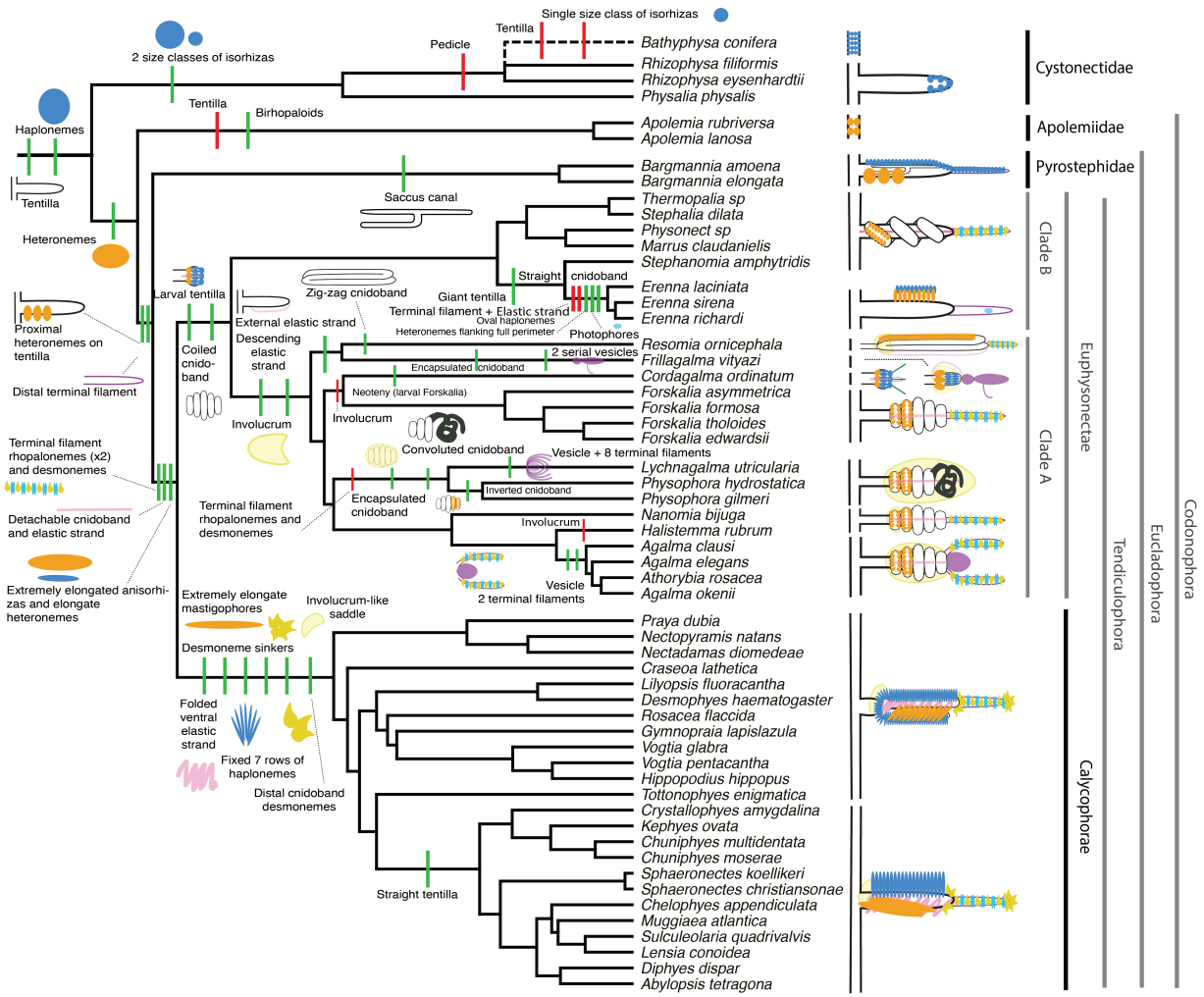


Figure 2: Siphonophore cladogram with the main categorical character gains (green) and losses (red) mapped. Some branch lengths were modified from the Bayesian chronogram to improve readability. The main visually distinguishable tentillum types are sketched next to the species that bear them, showing the location and arrangement of the main characters. In large, complex-shaped euphysonect tentilla, haplonemes were omitted for simplification. The hypothesized phylogenetic placement of the rhizophysid *Bathypysa conifera* branch was appended manually as a polytomy (dashed line).

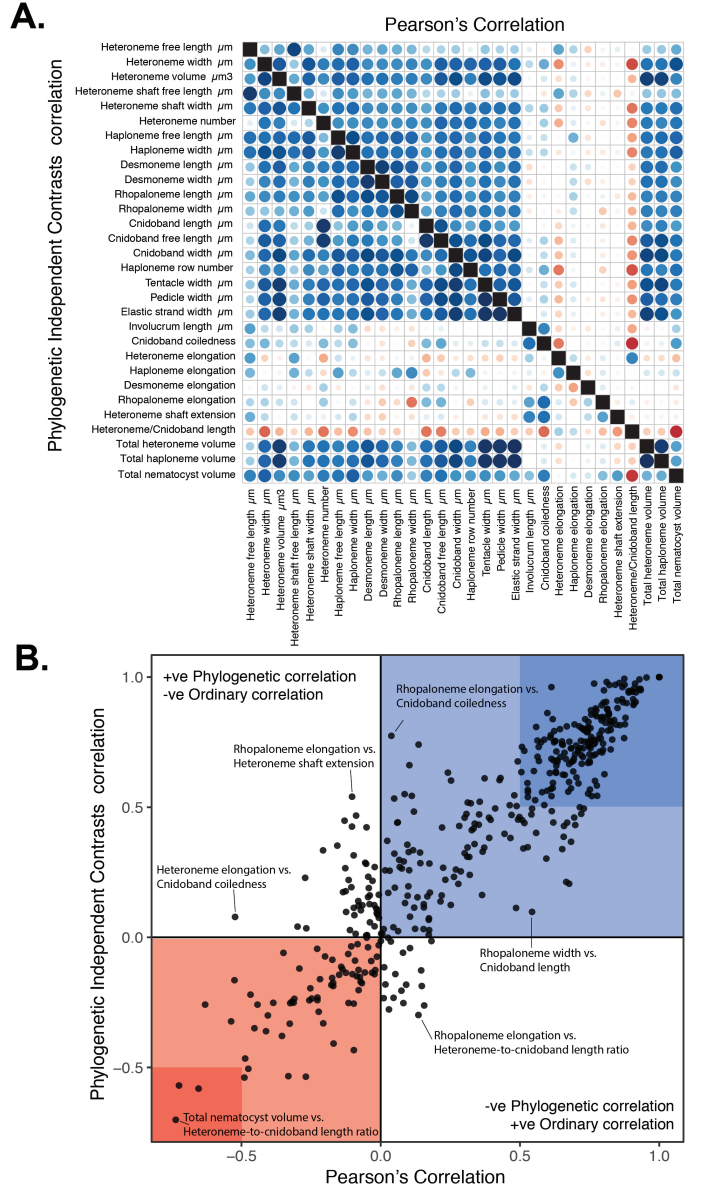


Figure 3: A. Correlogram showing strength of ordinary (upper triangle) and phylogenetic (lower triangle) correlations between characters. Both size and color of the circles indicate the strength of the correlation (R^2). B. Scatterplot of phylogenetic correlation against ordinary correlation showing a strong linear relationship ($R^2 = 0.92$, 95% confidence between 0.90 and 0.93). Light red and blue boxes indicate congruent negative and positive correlations respectively. Darker red and blue boxes indicate strong (<-0.5 or >0.5) negative and positive correlation coefficients respectively.

and Pyrostephidae. There is one secondary return to more oval, less elongated haplonemes in *Erenna*, but it does not reach the sphericity present in Cystonectae or Pyrostephidae (Fig. 4). Heteroneme evolution presents a less discrete evolutionary history, where Tendiculophora evolved more elongate heteronemes, but the difference between theirs and other siphonophores is much smaller than the variation in shape within Tendiculophora, bearing no phylogenetic signal. In this clade, the evolution of heteroneme shape has diverged in both directions, and there is no correlation with haploneme shape (Fig. 4), which has remained fairly constant (elongation between 1.5 and 2.5). Haploneme and heteroneme shape share 21% of their variance across extant values, and 53% of the variance in their shifts along the branches of the phylogeny. However, much of this correlation is due to the sharp contrast between Pyrostephidae and their sister group Tendiculophora. We searched for regime shifts in the evolution of haploneme nematocyst shape characters using a SURFACE (26). SURFACE identified seven distinct OU regimes in the evolutionary history of haploneme length and width (Fig. 7A). The different regimes are located (1) in cystonects, (2) in pyrostephids, (7) in apolemiids, (9) in *Erenna*, (6) in *Stephanomia*, (3) in most of Tendiculophora, (5) in *Cordagalma ordinatum*, (4) in most diphyomorphs, and (8) in *Abylopsis tetragona* and *Diphyes dispar*.

Phenotypic integration of the tentillum – Phenotypically integrated structures maintain evolutionary correlations between its constituent characters. Of the phylogenetic correlations (Fig. 3a, lower triangle), 81.3% were positive and 18.7% were negative, while of the ordinary correlations (Fig. 3a, upper triangle) 74.6% were positive and 25.4% were negative. Half (49.9%) of phylogenetic correlations were >0.5 , while only 3.6% are < -0.5 . Similarly, among the correlations across extant species, 49.1% were >0.5 and only 1.5% were < -0.5 . In addition, we found that 13.9% of character pairs had opposing phylogenetic and ordinary correlation coefficients. Just 4% have negative phylogenetic and positive ordinary correlations (such as rhopaloneme elongation ~ heteroneme-to-cnidoband length ratio and haploneme elongation, or haploneme elongation ~ heteroneme number), and only 9.9% of character pairs

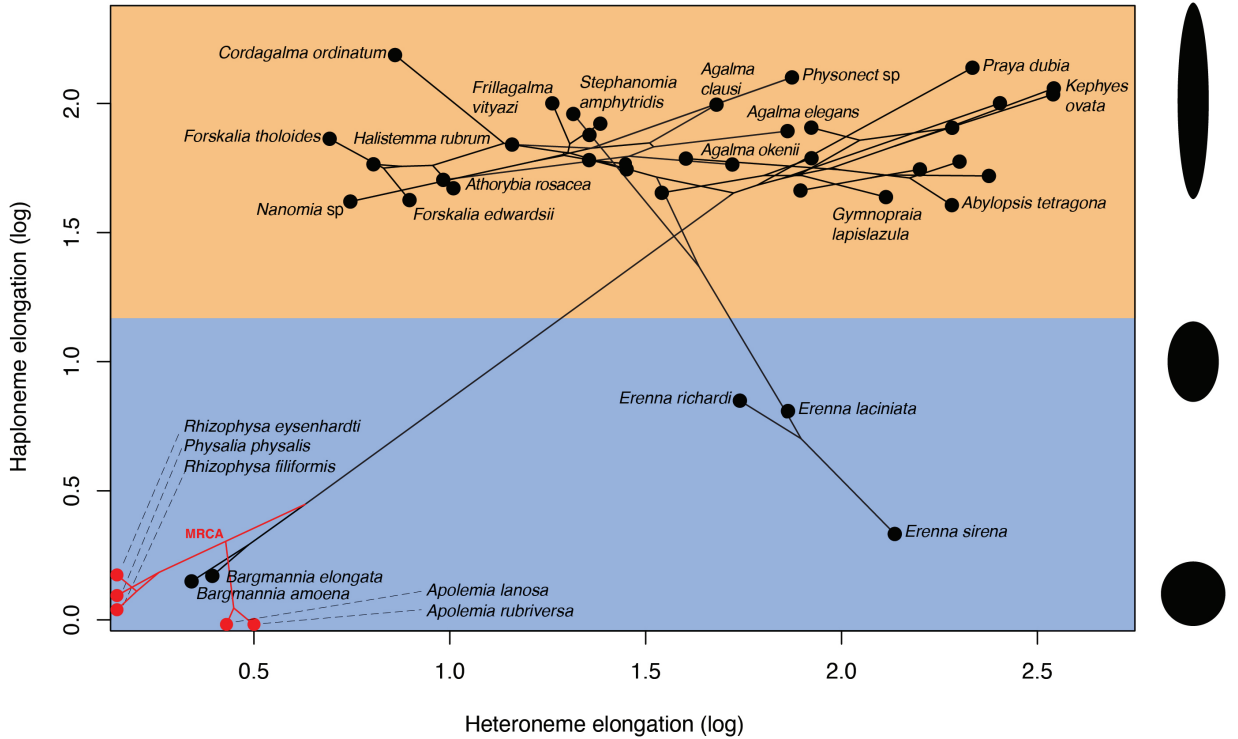


Figure 4: Phylomorphospace showing haploneme and heteroneme elongation (log scaled). Orange area delimits rod-shaped haplonemes, the blue area covers oval and round-shaped haplonemes. Smaller dots and lines represent phylogenetic relationships and ancestral states of internal nodes under BM. Species nodes in red lack either haplonemes or heteronemes, and their values are projected onto the axis of the nematocyst type they bear. Cystonects have no tentacle heteronemes and are projected onto the haploneme axis. Apolemiids have no tentacle haplonemes and are projected onto the heteroneme axis.

had positive phylogenetic correlation yet negative ordinary correlation (such as heteroneme elongation ~ cnidoband convolution and involucrum length, or rhopaloneme elongation with cnidoband length). These disparities could be explained by Simpson's paradox (31): the reversal of the sign of a relationship when a third variable (or a phylogenetic topology (32)) is considered. However, no character pair had correlation coefficient differences larger than 0.64 between ordinary and phylogenetic correlations (heteroneme shaft extension ~ rhopaloneme elongation has a Pearson's correlation of 0.10 and a phylogenetic correlation of -0.54). Rhopaloneme elongation shows the most incongruencies between phylogenetic and ordinary correlations with other characters. The phenotypic integration test showed significant integration signal between all modules, tentillum and haploneme modules sharing the greatest regression coefficient (SM12).

In the non-phylogenetic PCA morphospace using only **simple** characters (Fig. 5), PC1 (aligned with tentillum and tentacle size) explained 69.3% of the variation in the tentillum morphospace, whereas PC2 (aligned with heteroneme length, heteroneme number, and haploneme arrangement) explained 13.5%. In a phylogenetic PCA, 63% of the evolutionary variation in the morphospace is explained by PC1 (aligned with shifts in tentillum size), while 18% is explained by PC2 (aligned with shifts in heteroneme number and involucrum length).

Morphospace occupation – In order to examine the occupation structure of the morphospace across all siphonophore species in the dataset, we cast a PCA on the data after transforming inapplicable states (due to absence of character) to zeroes. This allows us to accommodate species with many missing characters (such as cystonects or apolemiids), and to account for common absences as morphological similarities. In this ordination, PC1 explains 47.45% of variation (aligned with cnidoband size) and PC2 explains 16.73% of variation (aligned with heteroneme volume and involucrum). When superimposing feeding guilds onto the morphospace (Fig. 6), we find that the morphospaces of each feeding guild are only slightly overlapping in PC1 and PC2. A phylogenetic MANOVA showed that feeding guilds explain 27.63% of variance across extant species (p value < 0.000001), and 20.97% of the variance

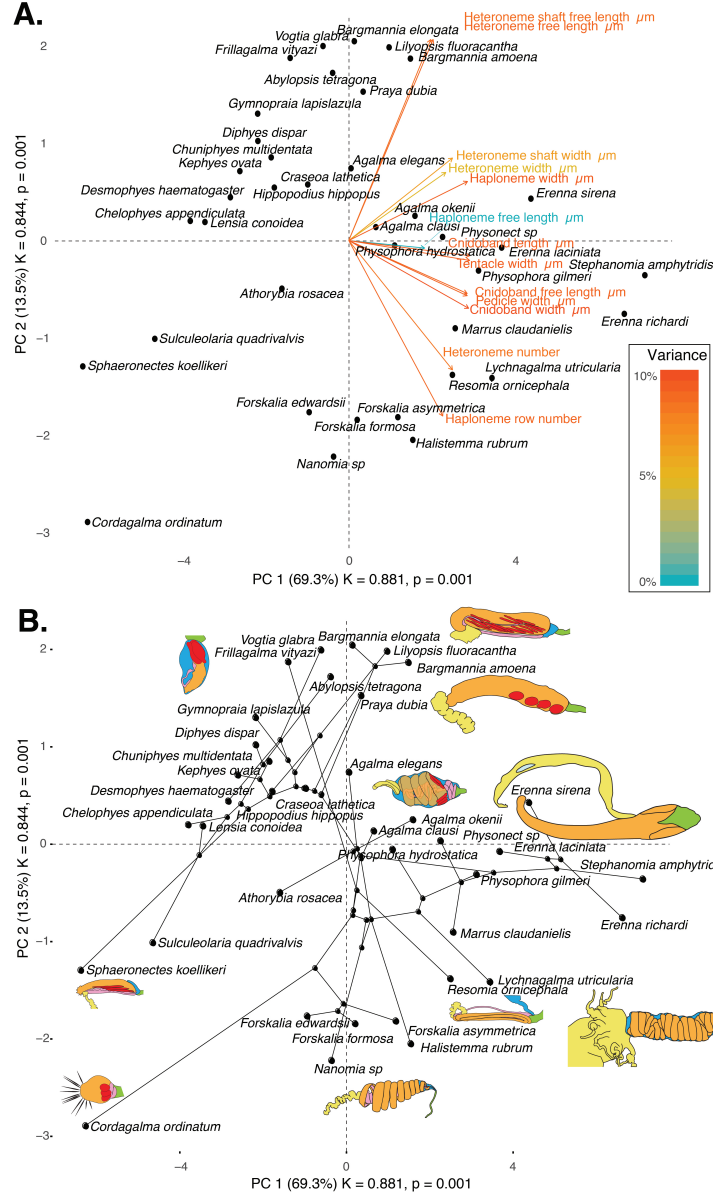


Figure 5: Phylomorphospace of the **simple** continuous characters principal components, excluding ratios and composite characters. A. Variance explained by each variable in the PC1-PC2 plane. Axis labels include the phylogenetic signal (K) for each component and p-value. B. Phylogenetic relationships between the species points distributed in that same space.

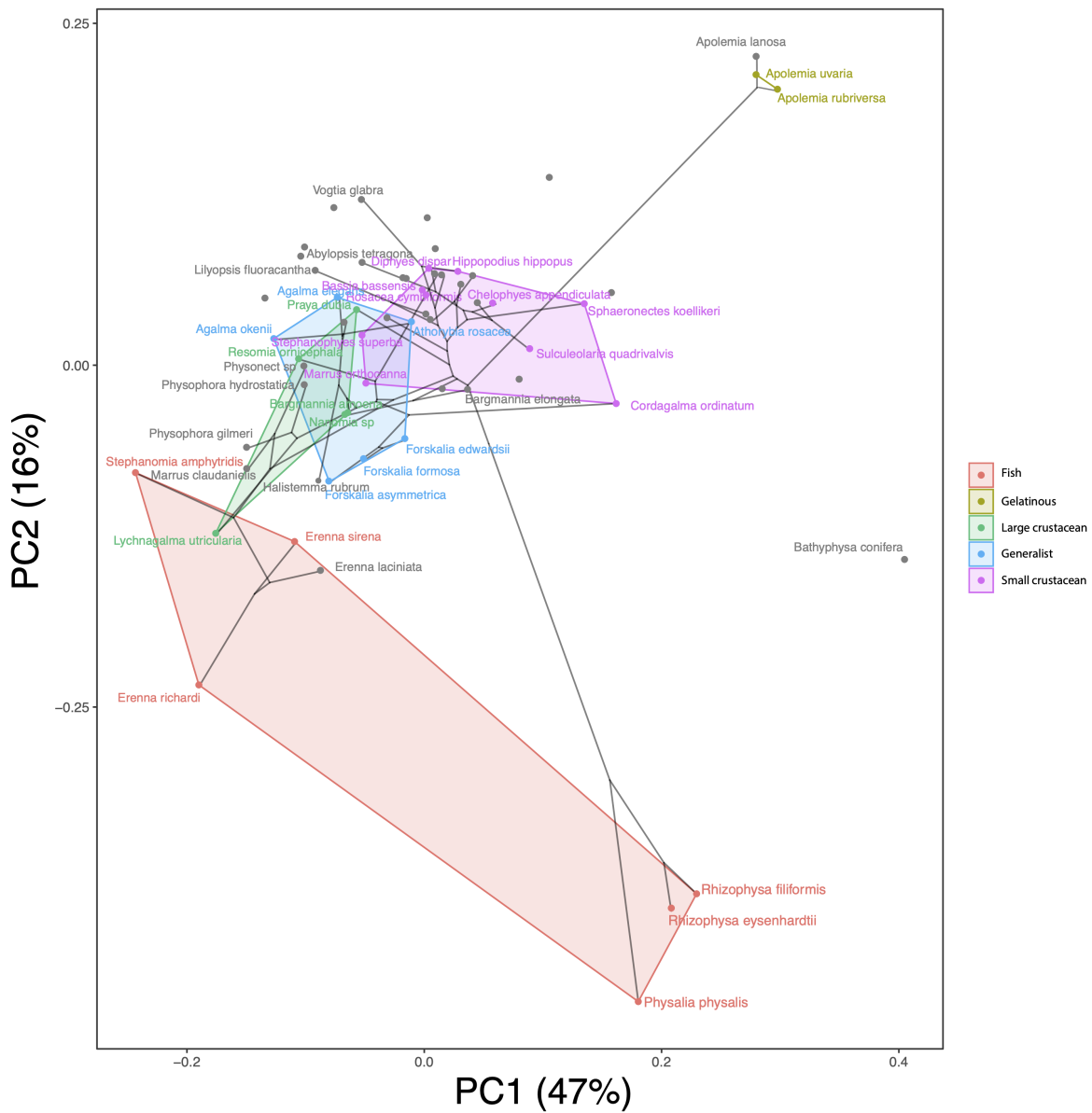


Figure 6: Phylomorphospace showing PC1 and PC2 from a PCA of continuous morphological characters with inapplicable states transformed to zeroes, overlapped with polygons conservatively defining the space occupied by each feeding guild. Lines between species coordinates show the phylogenetic relationships between them.

292 in the tree species accounting for phylogeny, an outcome significantly distinct from the
293 expectation under neutral evolution (p -value = 0.0196). In addition, a morphological disparity
294 analysis accounting for phylogenetic structure shows that the morphospace of fish specialists
295 is significantly broader than that of generalists and other specialists. This is due to the large
296 morphological disparities between cystonects and piscivorous euphysonects. There are no
297 significant differences among the morphospace disparities of the other feeding guilds.

298 *Convergent evolution* – Convergence is a widespread evolutionary phenomenon where dis-
299 tantly related clades independently evolve similar phenotypes. Using the package SURFACE
300 (26), we identified convergence in haploneme nematocyst shape and in morphospace position.
301 In (14), we identified haploneme nematocyst shape as one of the traits associated with the
302 convergent evolution of piscivory. Here we find that indeed wider haploneme nematocysts
303 have convergently evolved in the piscivore cytonects and *Erenna* spp. (Fig. 7A). Extremely
304 narrow haplonemes have also evolved convergently in *Cordagalma ordinatum* and copepod
305 specialist calycophorans such as *Sphaeronectes koellikeri*. When integrating many traits
306 into a couple principal components, we find two distinct convergences between euphysonects
307 and calycophorans with a reduced prey capture apparatus. Those convergences are between
308 *Frillagalma vityazi* and calycophorans, and once again between *Cordagalma ordinatum* and
309 *Sphaeronectes koellikeri* (Fig. 7B).

310 *Functional morphology of tentillum and nematocyst discharge* – Tentillum and nematocyst
311 discharge high speed measurements are available in the Dryad repository. While the sample
312 sizes of these measurements were insufficient to draw reliable statistical results at a phyloge-
313 netic level, we did observe patterns that may be relevant to their functional morphology. For
314 example, cnidoband length is strongly correlated with discharge speed (p value = 0.0002).
315 This is probably the sole driver of the considerable difference between euphysonect and
316 calycophoran tentilla discharge speeds (average discharge speeds: 225.0mm/s and 41.8mm/s
317 respectively; t-test p value = 0.011), since the euphysonects have larger tentilla than the
318 calycophorans among the species recorded. In addition, we observed that calycophoran

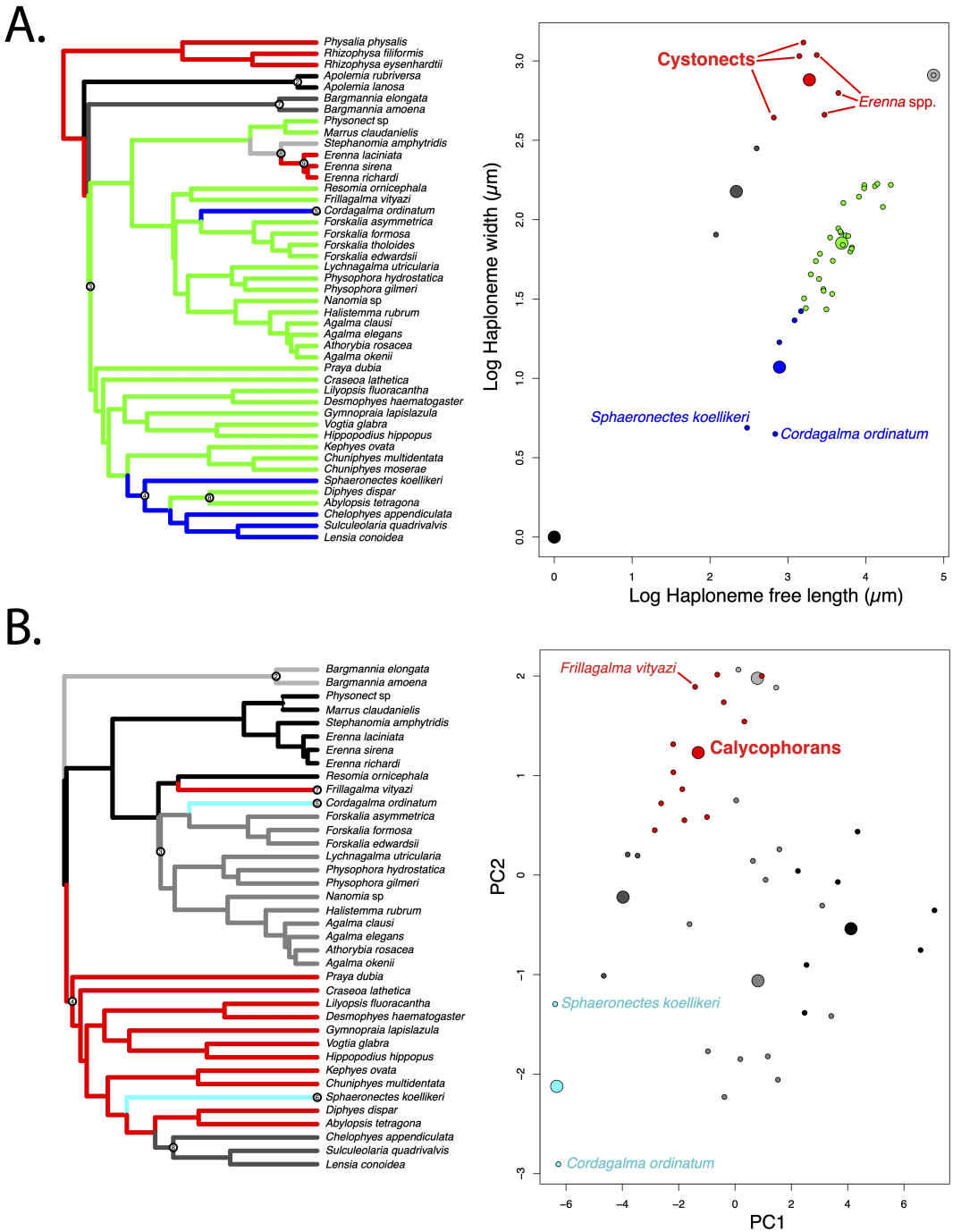


Figure 7: SURFACE plots showing convergent evolutionary regimes modelled under OU for (A) haploneme nematocyst length & width, and (B) for PC1 & 2 of all continuous characters with the exception of terminal filament nematocysts, and removing taxa with inapplicable character states. Node numbers on the tree label different regimes, regimes of the same color are identified as convergent. Small circles on the scatterplots indicate species values, large circles indicate the average position of the OU optima (θ) for a given combination of convergent regimes.

319 haploneme tubules fire faster than those of euphysonects (T -test p value = 0.001). Haploneme
320 nematocysts discharge 2.8x faster than heteroneme nematocysts (T -test p value = 0.0012).
321 Finally, we observed that the stenoteles of the Ephysonectae discharge a helical filament
322 that “drills” itself through the medium it penetrates as it everts.

323 *Generating dietary hypotheses using tentillum morphology* – For many siphonophore species,
324 no feeding observations have yet been published. To help bridge this gap of knowledge,
325 we generated hypotheses about the diets of these understudied siphonophores based on
326 their known tentacle morphology using **one** the linear discriminant analyses of principal
327 components (DAPC) fitted in (14). This provides concrete predictions to be tested in
328 future work and helps extrapolate our findings to many poorly known species that are
329 extremely difficult to collect and observe. The discriminant analysis for feeding guild (7
330 principal components, 4 discriminants) produced 100% discrimination, and the highest loading
331 contributions were found for the characters (ordered from highest to lowest): Involucrum
332 length, heteroneme volume, heteroneme number, total heteroneme volume, tentacle width,
333 heteroneme length, total nematocyst volume, and heteroneme width. We used the predictions
334 from this discriminant function to generate hypotheses about the feeding guild of 45 species
335 in the morphological dataset. This extrapolation predicts that two other *Apolemia* species are
336 gelatinous prey specialists like *Apolemia rubriversa*, and predicts that *Erenna laciniatais* a
337 fish specialist like *Erenna richardi*. When predicting soft- and hard-bodied prey specialization,
338 the DAPC achieved 90.9% discrimination success, only marginally confounding hard-bodied
339 specialists with generalists (SM13). The main characters driving this discrimination are
340 involucrum length, heteroneme number, heteroneme volume, tentacle width, total nematocyst
341 volume, total haploneme volume, elastic strand width, and heteroneme length.

342 Discussion

343 *On the evolution of tentilla morphology* – *On the evolution of tentilla morphology* – The
344 evolutionary rate covariance results in (14) indicate that tentilla are not only phenotypically

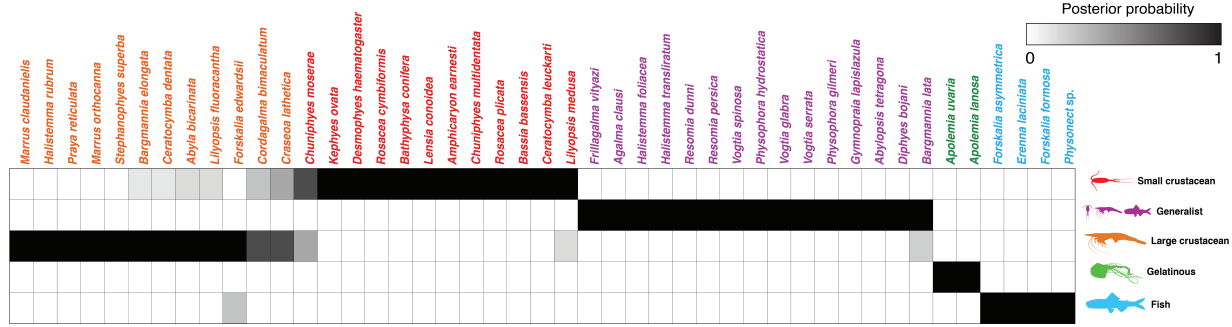


Figure 8: Hypothetical feeding guilds for siphonophore species predicted by a 6 PCA DAPC. Cell darkness indicates the posterior probability of belonging to each guild. Training data set transformed so inapplicable states are computed as zeroes. Species ordered and colored according to their predicted feeding guild.

integrated but also show patterns of evolutionary modularity, where different sets of characters appear to evolve in stronger correlations among each other than with other characters (33). This may be indicative of the underlying genetic and developmental dependencies among closely homologous nematocyst types (such as desmonemes and rhopalonemes) and structures. The rate covariance results are congruent with the evolutionary correlations we found (Fig. ??figure8)). In addition, these evolutionary modules point to hypothetical functional modules. For example, the coiling degree of the cnidoband and the extent of the involucrum have correlated rates of evolution, while high-speed videos (pers. obs.) show that the involucrum helps direct the whiplash of the uncoiling cnidoband distally (towards the prey). The clade Tendiculophora contains far more species than its relatives Cystonectae, Apolemiidae, and Pyrostephidae. An increase in clade richness and ecological diversification can be triggered by a ‘key innovation’ (34). The evolutionary innovation of the Tendiculophora tentilla with shooting cnidobands and modular regions may have facilitated further dietary diversification. A specific instance of this may have been the access to the abundant small crustacean prey such as copepods. The rapid darting escape response of copepods may preclude their capture in siphonophores without shooting cnidobands.

The siphonophore tentillum morphospace has a fairly low extant dimensionality due to having an evolutionary history with many synchronous, correlated changes. This is

363 consistent with strong phenotypic integration where genetic and developmental correlations
364 are maintained by natural selection to preserve a complex function across the wide variety
365 of morphologies present. Since most tentillum characters develop from a common bud
366 (budding tentilla near the base of the tentacle), structural correlations are expected. Similarly,
367 correlations between the features of different nematocyst subtypes within a species are also
368 expected given their common evolutionary and developmental origin (35, 36). However, we
369 also found correlations between nematocyst and tentillum characters. Siphonophore tentacle
370 nematocysts (in their cnidocytes) are not produced nor matured in the developing tentillum.
371 These cnidocytes are produced by dividing cnidoblasts in the basigaster (basal swelling of
372 the gastrozooid). Once the cnidocytes have assembled the nematocyst, they migrate outward
373 along the tentacle (37) and position themselves in the tentillum according to their type and size
374 (29). Thus, the developmental programs that produce the observed nematocyst morphologies
375 are spatially separated from those producing the tentillum morphologies. Therefore, we
376 hypothesize the genetic correlations and phenotypic integration between tentillum and
377 nematocyst characters are maintained through natural selection on separate regulatory
378 networks, out of the necessity to work together and meet the spatial, mechanical, and
379 functional constraints of their prey capture behavior.

380 *Heterochrony and convergence in the evolution of tentilla with diet* - In addition to
381 identifying shifts in prey type, (14) revealed the specific morphological changes in the prey
382 capture apparatus associated with these changes. Copepod-specialized diets have evolved
383 independently in *Cordagalma* and some calycophorans. These evolutionary transitions
384 happened together with transitions to smaller tentilla with fewer and smaller cnidoband
385 nematocysts. We found that these morphological transitions evolved convergently in these
386 taxa. Tentilla are expensive single-use structures (16), therefore we would expect that
387 specialization in small prey would beget reductions in the size of the prey capture apparatus
388 to the minimum required for the ecological performance. Such a reduction in size would
389 require extremely fast rates of trait evolution in an ordinary scenario. However, *Cordagalma*'s

³⁹⁰ tentilla strongly resemble the larval tentilla (only found in the first-budded feeding body of
³⁹¹ the colony) of their sister genus *Forskalia*. This indicates that the evolution of *Cordagalma*
³⁹² tentilla could be a case of paedomorphic heterochrony associated with predatory specialization
³⁹³ on smaller prey. This developmental shift may have provided a shortcut for the evolution of
³⁹⁴ a smaller prey capture apparatus.

³⁹⁵ Our work identifies yet another novel example of convergent evolution. The region of
³⁹⁶ the tentillum morphospace (Fig. 5 & Fig. ??surface)B) occupied by calycophorans was
³⁹⁷ independently (and more recently) occupied by the physonect *Frillagalma vityazi*. Like
³⁹⁸ calycophorans, *Frillagalma* tentilla have small C-shaped cnidobands with a few rows of
³⁹⁹ anisorhizas. Unlike calycophorans, they lack paired elongate microbasic mastigophores.
⁴⁰⁰ Instead, they bear exactly three oval stenoteles, and their cnidobands are followed by a
⁴⁰¹ branched vesicle, unique to this genus. Their tentillum morphology is very different from
⁴⁰² that of other related physonects, which tend to have long, coiled, cnidobands with many
⁴⁰³ paired oval stenoteles. Our SURFACE analysis clearly indicates a regime convergence in the
⁴⁰⁴ cnidoband morphospace between *Frillagalma* and calycophorans (Fig. 7B). Most studies on
⁴⁰⁵ calycophoran diets have reported their prey to be primarily composed of small crustaceans,
⁴⁰⁶ such as copepods or ostracods (17, 38). The diet of *Frillagalma vityazi* is unknown, but this
⁴⁰⁷ morphological convergence suggests that they evolved to capture similar kinds of prey. The
⁴⁰⁸ DAPCs in (14) predict that *Frillagalma* has a generalist niche with both soft and hard-bodied
⁴⁰⁹ prey, including copepods.

⁴¹⁰ *Evolution of nematocyst shape* – A remarkable feature of siphonophore haplonemes is
⁴¹¹ that they are outliers to all other Medusozoa in their surface area to volume relationships,
⁴¹² deviating significantly from sphericity (39). This suggests a different mechanism for their
⁴¹³ discharge that could be more reliant on capsule tension than on osmotic potentials (40), and
⁴¹⁴ strong selection for efficient nematocyst packing in the cnidoband (29, 39). Our results show
⁴¹⁵ that Codonophora underwent a shift towards elongation and Cystonectae towards sphericity,
⁴¹⁶ assuming the common ancestor had an intermediate state. Since we know that the haplonemes

417 of other hydrozoan outgroups are generally spheroid, it is more parsimonious to assume that
418 cystonects are simply retaining this ancestral state. Later, we observe a return to more
419 rounded (ancestral) haplonemes in *Erenna*, concurrent with a secondary gain of a piscivorous
420 trophic niche, like that exhibited by cystonects. Our SURFACE analysis shows that this
421 transition to roundness is convergent with the regime occupied by cystonects (Fig. 7A).
422 Purcell (38) showed that haplonemes have a penetrating function as isorhizas in cystonects
423 and an adhesive function as anisorhizas in Tendiculophora. It is no coincidence that the two
424 clades that have converged to feed primarily on fish have also converged morphologically
425 toward more compact haplonemes. Isorhizas in cystonects are known to penetrate the skin of
426 fish during prey capture, and to deliver the toxins that aid in paralysis and digestion (41).
427 *Erenna*'s anisorhizas are also able to penetrate human skin and deliver a painful sting (4)
428 (and pers. obs.), a common feature of piscivorous cnidarians like the Portuguese man-o-war
429 or box jellies.

430 The implications of these results for the evolution of nematocyst function are that an
431 innovation in the discharge mechanism of haplonemes may have occurred during the main shift
432 to elongation. Elongate nematocysts can be tightly packed into cnidobands. We hypothesize
433 this may be a Tendiculophora lineage-specific adaptation to packing more nematocysts into a
434 limited tentillum space, as suggested by (29). Thomason (39) hypothesized that smaller, more
435 spherical nematocysts, with a lower surface area to volume ratio, are more efficient in osmotic-
436 driven discharge and thus have more power for skin penetration. The elongated haplonemes
437 of crustacean-eating Tendiculophora have never been observed penetrating their crustacean
438 prey (38), and are hypothesized to entangle the prey through adhesion of the abundant
439 spines to the exoskeletal surfaces and appendages. Entangling requires less acceleration and
440 power during discharge than penetration, as it does not rely on point pressure. In fish-eating
441 cystonects and *Erenna* species, the haplonemes are much less elongated and very effective at
442 penetration, in congruence with the osmotic discharge hypothesis. Tendiculophora, composed
443 of the clades Euphysonectae and Calycophorae, includes the majority of siphonophore species.

444 Within these clades are the most abundant siphonophore species, and a greater morphological
445 and ecological diversity is found. We hypothesize that this packing-efficient haploneme
446 morphology may have also been a key innovation leading to the diversification of this clade.
447 However, other characters that shifted concurrently in the stem of this clade could have been
448 equally responsible for their extant diversity.

449 *Generating hypotheses on siphonophore feeding ecology* – One motivation for our research
450 is to understand the links between **predator capture tools** and their diets so we can generate
451 hypotheses about the diets of siphonophores based on morphological characteristics. Indeed,
452 our discriminant analyses were able to distinguish between different siphonophore diets
453 based on morphological characters alone. The models produced by these analyses generated
454 testable predictions about the diets of many species for which we only have morphological
455 data of their tentacles. While the limited dataset used here is informative for generating
456 tentative hypotheses, the empirical dietary data are still scarce and insufficient to cast robust
457 predictions. This reveals the need to extensively characterize siphonophore diets and feeding
458 habits. In future work, we will test these ecological hypotheses and validate these models
459 by directly characterizing the diets of some of those siphonophore species. Predicting diet
460 using morphology is a powerful tool to reconstruct food web topologies from community
461 composition alone. In many of the ecological models found in the literature, interactions
462 among the oceanic zooplankton have been treated as a black box (42). The ability to predict
463 such interactions, including those of siphonophores and their prey, will enhance the taxonomic
464 resolution of nutrient-flow models constructed from plankton community composition data.

465 Acknowledgements

466 This work was supported by the Society of Systematic Biologists (Graduate Student Award
467 to A.D.S.); the Yale Institute of Biospheric Studies (Doctoral Pilot Grant to A.D.S.); and
468 the National Science Foundation (Waterman Award to C.W.D., and NSF-OCE 1829835 to
469 C.W.D., S.H.D.H., and C. Anela Choy). A.D.S. was supported by a Fulbright Spain Graduate

⁴⁷⁰ Studies Scholarship.

⁴⁷¹ References

- ⁴⁷² 1. Pugh P (1983) *Benthic siphonophores: A review of the family rhodaliidai (siphonophora, physonectae)* (Royal Society).
- ⁴⁷⁴ 2. Pugh P, Harbison G (1986) New observations on a rare physonect siphonophore, *lychnagalma utricularia* (claus, 1879). *Journal of the Marine Biological Association of the United Kingdom* 66(3):695–710.
- ⁴⁷⁷ 3. Pugh P, Youngbluth M (1988) Two new species of prayine siphonophore (calycophorae, prayidae) collected by the submersibles johnson-sea-link i and ii. *Journal of Plankton Research* 10(4):637–657.
- ⁴⁸⁰ 4. Pugh P (2001) A review of the genus *erenna bedot*, 1904 (siphonophora, physonectae). *BULLETIN-NATURAL HISTORY MUSEUM ZOOLOGY SERIES* 67(2):169–182.
- ⁴⁸² 5. Hissmann K (2005) In situ observations on benthic siphonophores (physonectae: Rhodaliidae) and descriptions of three new species from indonesia and south africa. *Systematics and Biodiversity* 2(3):223–249.
- ⁴⁸⁵ 6. Haddock SH, Dunn CW, Pugh PR (2005) A re-examination of siphonophore terminology and morphology, applied to the description of two new prayine species with remarkable bio-optical properties. *Journal of the Marine Biological Association of the United Kingdom* 85(3):695–707.
- ⁴⁸⁹ 7. Dunn CW, Pugh PR, Haddock SH (2005) *Marrus claudanielis*, a new species of deep-sea physonect siphonophore (siphonophora, physonectae). *Bulletin of Marine Science* 76(3):699–714.
- ⁴⁹² 8. Bardi J, Marques AC (2007) Taxonomic redescription of the portuguese man-of-war, *physalia physalis* (cnidaria, hydrozoa, siphonophorae, cystonectae) from brazil. *Iheringia Série Zoologia* 97(4):425–433.
- ⁴⁹⁵ 9. Pugh P, Haddock S (2010) Three new species of remosiid siphonophore (siphonophora:

- 496 Physonectae). *Journal of the Marine Biological Association of the United Kingdom* 90(6):1119–
497 1143.
- 498 10. Pugh P, Baxter E (2014) A review of the physonect siphonophore genera halistemma
499 (family agalmatidae) and stephanomia (family stephanomiidae). *Zootaxa* 3897(1):1–111.
- 500 11. Totton AK, Bargmann HE (1965) *A synopsis of the siphonophora* (British Museum
501 (Natural History)).
- 502 12. Mapstone GM (2014) Global diversity and review of siphonophorae (cnidaria: Hydro-
503 zoa). *PLoS One* 9(2):e87737.
- 504 13. Munro C, et al. (2018) Improved phylogenetic resolution within siphonophora
505 (cnidaria) with implications for trait evolution. *Molecular Phylogenetics and Evolution*.
- 506 14. Damian-Serrano A, Haddock SH, Dunn CW (2019) The evolution of siphonophore
507 tentilla as specialized tools for prey capture. *bioRxiv*:653345.
- 508 15. Mariscal RN (1974) Nematocysts.
- 509 16. Mackie GO, Pugh PR, Purcell JE (1987) Siphonophore Biology. *Advances in Marine
510 Biology* 24:97–262.
- 511 17. Purcell J (1981) Dietary composition and diel feeding patterns of epipelagic
512 siphonophores. *Marine Biology* 65(1):83–90.
- 513 18. Harmon LJ, Weir JT, Brock CD, Glor RE, Challenger W (2007) GEIGER: Investi-
514 gating evolutionary radiations. *Bioinformatics* 24(1):129–131.
- 515 19. Sugiura N (1978) Further analysts of the data by akaike's information criterion
516 and the finite corrections: Further analysts of the data by akaike's. *Communications in
517 Statistics-Theory and Methods* 7(1):13–26.
- 518 20. Pennell MW, FitzJohn RG, Cornwell WK, Harmon LJ (2015) Model adequacy and the
519 macroevolution of angiosperm functional traits. *The American Naturalist* 186(2):E33–E50.
- 520 21. Blomberg SP, Garland T, Ives AR (2003) Testing for phylogenetic signal in comparative
521 data: Behavioral traits are more labile. *Evolution* 57(4):717–745.
- 522 22. Revell LJ (2012) Phytools: An r package for phylogenetic comparative biology (and

- 523 other things). *Methods in Ecology and Evolution* 3(2):217–223.
- 524 23. Felsenstein J (1985) Phylogenies and the comparative method. *The American*
525 *Naturalist* 125(1):1–15.
- 526 24. Revell LJ, Chamberlain SA (2014) Rphylip: An r interface for phylip. *Methods in*
527 *Ecology and Evolution* 5(9):976–981.
- 528 25. Adams DC, Collyer M, Kaliontzopoulou A, Sherratt E (2016) Geomorph: Software
529 for geometric morphometric analyses.
- 530 26. Ingram T, Mahler DL (2013) SURFACE: Detecting convergent evolution from
531 comparative data by fitting ornstein-uhlenbeck models with stepwise akaike information
532 criterion. *Methods in ecology and evolution* 4(5):416–425.
- 533 27. Jombart T, Devillard S, Balloux F (2010) Discriminant analysis of principal compo-
534 nents: A new method for the analysis of genetically structured populations. *BMC genetics*
535 11(1):94.
- 536 28. Siebert S, Pugh PR, Haddock SH, Dunn CW (2013) Re-evaluation of characters in
537 apolemiidae (siphonophora), with description of two new species from monterey bay, california.
538 *Zootaxa* 3702(3):201–232.
- 539 29. Skaer R (1988) *The formation of cnidocyte patterns in siphonophores* (Academic
540 Press New York).
- 541 30. Skaer R (1991) Remodelling during the development of nematocysts in a siphonophore.
542 *Hydrobiologia* (Springer), pp 685–689.
- 543 31. Blyth CR (1972) On simpson’s paradox and the sure-thing principle. *Journal of the*
544 *American Statistical Association* 67(338):364–366.
- 545 32. Uyeda JC, Zenil-Ferguson R, Pennell MW (2018) Rethinking phylogenetic comparative
546 methods. *Systematic Biology* 67(6):1091–1109.
- 547 33. Wagner GP (1996) Homologues, natural kinds and the evolution of modularity.
548 *American Zoologist* 36(1):36–43.
- 549 34. Simpson GG (1955) *Major features of evolution* (Columbia University Press: New

- 550 York).
- 551 35. Bode H (1988) Control of nematocyte differentiation in hydra. *The Biology of*
552 *Nematocysts* (Elsevier), pp 209–232.
- 553 36. David CN, et al. (2008) Evolution of complex structures: Minicollagens shape the
554 cnidarian nematocyst. *Trends in genetics* 24(9):431–438.
- 555 37. Carré D (1972) Study on development of cnidocysts in gastrozooids of muggiaeae kochi
556 (will, 1844) (siphonophora, calycophora). *Comptes Rendus Hebdomadaires des Seances de*
557 *l'Academie des Sciences Serie D* 275(12):1263.
- 558 38. Purcell JE (1984) The functions of nematocysts in prey capture by epipelagic
559 siphonophores (coelenterata, hydrozoa). *The Biological Bulletin* 166(2):310–327.
- 560 39. Thomason J (1988) The allometry of nematocysts. *The Biology of Nematocysts*
561 (Elsevier), pp 575–588.
- 562 40. Carré D, Carré C (1980) On triggering and control of cnidocyst discharge. *Marine &*
563 *Freshwater Behaviour & Phy* 7(1):109–117.
- 564 41. Hessinger DA (1988) Nematocyst venoms and toxins. *The Biology of Nematocysts*
565 (Elsevier), pp 333–368.
- 566 42. Mitra A (2009) Are closure terms appropriate or necessary descriptors of zooplankton
567 loss in nutrient–phytoplankton–zooplankton type models? *Ecological Modelling* 220(5):611–
568 620.